Control and Cybernetics

vol. **40** (2011) No. 3

Numerical experiments with model equations of cancer invasion of tissue*†

by

Mikhail Kolev[1] and Barbara Zubik-Kowal[2]

[1] Faculty of Mathematics and Computer Science,
University of Warmia and Mazury
Słoneczna 54, 10-710 Olsztyn, Poland

[2] Department of Mathematics, Boise State University
1910 University Drive, Boise, Idaho 83725, USA

e-mail: kolev@matman.uwm.edu.pl, zubik@math.boisestate.edu

Abstract: In this paper we investigate a mathematical model of cancer invasion of tissue, which incorporates haptotaxis, chemotaxis, proliferation and degradation rates for cancer cells and the extracellular matrix, kinetics of urokinase receptor, and urokinase plasminogen activator cycle. We solve the model using spectrally accurate approximations and compare its numerical solutions with laboratory data. The spectral accuracy allows to use low-dimensional matrices and vectors, which speeds up the computations of the numerical solutions and thus to estimate the parameter values for the model equations. Our numerical results demonstrate correlations between numerical data computed from the mathematical model and *in vivo* tumour growth rates from prostate cell lines.

Keywords: *in vivo* tumorigenicity, cancer cells, proliferation, chemotaxis, haptotaxis, extracellular matrix, tumour invasion, mathematical model, animal models, approximations.

1. Introduction

Animal models prove useful to researchers in the manipulation of specific aspects of cancerogenic systems and for the testing of experimental therapies (see Holzer et al., 2003). On the other hand, mathematical models demonstrate potential to provide alternatives to animal models and decrease the numbers of

*Submitted: September 2010; Accepted: August 2011.

†This is an extended and amended version of the paper, presented at the 5$^{\text{th}}$ Congress of Young IT Scientists (Międzyzdroje, 23-25.IX.2010).

laboratory experiments and partially replace them by numerical experiments, which describe the behaviour of simulated tumours.

The purpose of the paper is to use the laboratory data from Calvo et al. (2002) and compute parameter values for the mathematical model of cancer invasion of tissue, which includes differential equations for kinetics of urokinase receptor and urokinase plasminogen activator cycle, and incorporates haptotaxis, chemotaxis, and proliferation and degradation rates for cancer cells and the extracellular matrix (see Chaplain and Lolas, 2006). We estimate the parameter values for the model equations by minimizing the error between the computed solutions and the available laboratory data.

In Jackiewicz et al. (2009), the laboratory data from Calvo et al. (2002) were successfully applied to estimate parameter values for the kinetic model by Kolev (2005), which is composed of partial integro-differential equations. The application of models of this type to tumour growth has been initiated by Bellomo and Forni (1994) and developed later in a series of papers (e.g. De Lillo et al., 2007; Bellomo and Delitala, 2008; Bellomo, Li and Maini, 2008; De Angelis and Lodz, 2008). Recently, Lachowicz (2005) has proved that, for certain parameter ranges, a particular kinetic model considered on infinite domains is equivalent to the macroscopic model by Chaplain and Anderson (2003). The result by Lachowicz (2005) was a motivation for the parameter estimation in Kolev and Zubik-Kowal (2010) for the model by Chaplain and Anderson (2003). Since the latter model does not include differential equations describing kinetics of urokinase receptor and urokinase plasminogen activator cycle, in this paper, we apply the laboratory data from Calvo et al. (2002) to the macroscopic model by Chaplain and Lolas (2006), which is different than the models in Chaplain and Anderson (2003) and Kolev (2005). The parameter values for the macroscopic model by Chaplain and Lolas (2006), with differential equations describing kinetics of urokinase receptor and urokinase plasminogen activator cycle, were not yet estimated according to laboratory data.

For the estimation of the parameter values for the model by Chaplain and Lolas (2006), we construct a numerical algorithm based on spectrally accurate approximations. The approximations allow to use low-dimensional vectors of data for solving the model and save computational time for each solution computed for the selection of the parameter values. We use the approximations to gain model parameters for five cell lines and compute the numerical data for the corresponding growths of tumours. Results concerning errors of the spectrally accurate approximations, which we apply in this paper, are provided in the book by Canuto et al. (1988). The book by Fornberg (1996) also provides many illustrations, examples, explanations, comparisons of approximations, and error estimates for spectral methods. Additionally, it shows significant strengths of spectral approximations in solving time-dependent PDEs. The book by Fornberg (1996) also presents applications of spectral approximations in turbulence modelling, weather prediction, and wave motion. Our paper shows that spectral approximations can also be applied in cancer research.

The paper is organized as follows. A mathematical description of the model equations is provided in Section 2. In Section 3, we introduce the numerical algorithm and present numerical experiments that lead to parameter estimation for the model equations and comparison of the resulting numerical solutions with the laboratory data. Finally, Section 4 includes our concluding remarks and future directions.

2. Oscillatory behaviour in cancer cells and extracellular matrix proliferation terms

In this paper, we apply laboratory data and find parameter values for the mathematical model, which was introduced by Chaplain and Lolas (2006). The objective of the paper is to demonstrate that the model by Chaplain and Lolas (2006) has the potential to describe the behaviour of cell populations *in vivo* and to predict growths of tumours. In this paper, we have obtained a correspondence between predicted and laboratory data. We computed the predicted data from the model by Chaplain and Lolas (2006) and present them in the next section. The data are compared with laboratory data in Fig. 1.

For the cancer cell motion, Chaplain and Lolas (2006) considered the following partial differential equation:

$$\frac{\partial n}{\partial t} = \underbrace{\frac{\partial}{\partial x}\Big(d_n \frac{\partial n}{\partial x}\Big)}_{dispersion} - \underbrace{\frac{\partial}{\partial x}\Big(\chi n \frac{\partial m}{\partial x}\Big)}_{chemotaxis} - \underbrace{\frac{\partial}{\partial x}\Big(\gamma n \frac{\partial f}{\partial x}\Big)}_{haptotaxis} + \underbrace{\mu_1 np(1-n-f)}_{proliferation}, \quad (2.1)$$

where the tumour cell density n depends on time t and the spatial variable x from the scaled domain $[0,1]$. Moreover, d_n is the random motility coefficient, μ_1 is the proliferation rate of the tumour cells, and χ and γ are the chemotactic and haptotactic coefficients, respectively. The proliferation of tumour cells is modelled by the term $\mu_1 pn(1-n-f)$, which, because of p, the concentration of the urokinase plasminogen activator (uPA) bound to the uPA receptor (uPAR), allows to incorporate the oscillatory behaviour in the cancer cells, see Chaplain and Lolas (2006). The unknown functions f and m represent the density of the extracellular matrix (ECM) and uPA concentration, respectively.

The extracellular matrix is a complex meshwork of proteins and proteoglycans that isolates tissue compartments, within which solid organs are placed (see Liotta et al., 1983). The equation governing the processes of the ECM degradation and production is the following equation:

$$\frac{\partial f}{\partial t} = - \underbrace{\eta m f}_{proteolysis} + \underbrace{\mu_2 fp(1-n-f)}_{renewal}, \quad (2.2)$$

where η and μ_2 are the rate constants for the degradation and growth, respectively. Motivated by the information on clinical observations of the increased

production (re-establishment) of ECM in case of prostate cancer (see Liotta et al., 1983), we consider the model with $\mu_2 \neq 0$.

Proteases such as metalloproteases and serine proteases are enzymes that are released from tumours. They play very significant role in the degradation of ECM thus allowing the migration of cancer cells and their metastasis. The serine proteases of the plasminogen activation system include urokinase uPA, which uses a specific uPA receptor (uPAR) to migrate through the ECM (see Andreasen et al., 1997, 2000). The uPA is produced by the tumour cells, diffuses throughout the tissue, and undergoes decay. Therefore, the equation governing the evolution of uPA concentration is given by

$$\frac{\partial m}{\partial t} = \underbrace{d_m \frac{\partial^2 m}{\partial x^2}}_{diffusion} + \underbrace{\alpha n}_{production} - \underbrace{\beta m}_{decay}, \tag{2.3}$$

where d_m is a constant diffusion coefficient, α is the production rate, and β is the decay rate.

As in Chaplain and Lolas (2006), we choose the following system of ordinary differential equations for the uPAR kinetics:

$$\begin{aligned} \frac{dp}{dt} &= q - 3 \\ \frac{dq}{dt} &= (q-3)\Big(1 - (p-2.1)^2\Big) - (p - 2.1), \end{aligned} \tag{2.4}$$

where q represents the concentration of the uPAR. Figure 18 in Chaplain and Lolas (2006), illustrates the limit cycle kinetics of the system (2.4). The combined system (2.1)-(2.4) overcomes the weakness of the models, which incorporate only constant reduction terms for cancer cells.

The system (2.1)-(2.4) is not complete and has to be closed by initial and boundary conditions. As in Chaplain and Anderson (2003) and Chaplain and Lolas (2006), we assume that at time $t = 0$, the initial small lump of cancer cells is centered around $x = 0$ and the function n has the initial Gaussian distribution

$$n(x, 0) = \exp\big(-x^2/\epsilon\big), \tag{2.5}$$

where ϵ is a positive constant. For the initial distribution of ECM and uPA we choose

$$\begin{aligned} f(x, 0) &= 1 - 0.5n(x, 0), \\ m(x, 0) &= 0.5n(x, 0), \end{aligned} \tag{2.6}$$

where $x \in [0, 1]$, see Chaplain and Anderson (2003), and we choose $p(0)$ and $q(0)$ according to numerical experiments and laboratory data. For the boundary

conditions we choose the zero-flux conditions

$$\frac{\partial n}{\partial x}(0,t) = \frac{\chi}{d_n} n(0,t) \frac{\partial m}{\partial x}(0,t) + \frac{\gamma}{d_n} n(0,t) \frac{\partial f}{\partial x}(0,t), \qquad \frac{\partial m}{\partial x}(0,t) = 0 \tag{2.7}$$

at the left edge $x = 0$ (the condition (2.6) is denoted in Chaplain and Lolas (2006) by (8) and the condition (2.7) is denoted in Chaplain and Lolas (2006) by (6)-(7)), and the Dirichlet conditions

$$n(1,t) = 0, \qquad m(1,t) = 0, \tag{2.8}$$

at the right edge $x = 1$ of the considered part of the tissue, which abuts a healthy part of the organism at $x = 1$.

The purpose of this paper is to apply the experimental data from Calvo et al. (2002) to the model (2.1)-(2.8) and demonstrate that its solutions correlate with the *in vivo* growths of prostate tumours tested in five nude mice (see Calvo et al., 2002). In the next section, we construct a numerical algorithm for the model (2.1)-(2.8) and compute its parameters $\mu_1, \mu_2, \alpha, \beta, \gamma, \eta, \chi, d_n, d_m$ by minimizing the error between its numerical solutions and the experimental data from Calvo et al. (2002). Since the solutions have to be computed for many different sets of the parameters, we construct the algorithm by using spectrally accurate approximations so that the resulting schemes are based on small amounts of spatial grid-points and low-dimensional vectors, which saves computational time for each solution corresponding to one combination of the parameters. Thanks to the spectral accuracy we found such parameter values of the model equations for which the resulting numerical data correlate with the laboratory data.

3. Numerical algorithm

In this section, we describe the numerical algorithm, which we apply to the model (2.1)-(2.4). Consider the Chebyshev-Gauss-Lobatto points

$$x_i = \frac{1}{2} - \frac{1}{2} \cos \frac{i\pi}{N+1}, \tag{3.1}$$

with $i = 0, 1, \ldots, N+1$ and the first order differentiation matrix

$$D = \left[d_{i,j} \right]_{i,j=0}^{N+1}$$

based on (3.1). The entries $d_{i,j}$ are defined by the expressions

$$d_{i,j} = \begin{cases} \dfrac{c_i}{c_j}\dfrac{(-1)^{i+j}}{x_i - x_j}, & i \neq j, \\ -\dfrac{x_j}{2(1-x_j^2)}, & 1 \leq i = j \leq N, \\ \dfrac{2(N+1)^2+1}{6}, & i = j = 0, \\ -\dfrac{2(N+1)^2+1}{6}, & i = j = N+1, \end{cases}$$

where

$$c_i = \begin{cases} 2, & i = 0, N+1, \\ 1, & i = 1, \ldots, N, \end{cases}$$

see Canutp et al. (1998).

We note that the word *matrix* is used here in the mathematical sense (as e.g. in Canuto (1998) and Fornberg (1996)) as an array of quantities or expressions in rows and columns. On the other hand, before Section 3, we use the word *matrix* (ECM-ExtraCellular Matrix) in the biological sense as e.g. in Chaplain and Anderson (2003) and Chaplain and Lolas (2006).

We use the following notations

$$n(t) = \begin{bmatrix} n(x_0,t) \\ n(x_1,t) \\ \vdots \\ n(x_N,t) \end{bmatrix}, \quad n_x(t) = \begin{bmatrix} \dfrac{\partial n}{\partial x}(x_0,t) \\ \dfrac{\partial n}{\partial x}(x_1,t) \\ \vdots \\ \dfrac{\partial n}{\partial x}(x_N,t) \end{bmatrix}, \quad n_{xx}(t) = \begin{bmatrix} \dfrac{\partial^2 n}{\partial x^2}(x_0,t) \\ \dfrac{\partial^2 n}{\partial x^2}(x_1,t) \\ \vdots \\ \dfrac{\partial^2 n}{\partial x^2}(x_N,t) \end{bmatrix},$$

and similar notations for f and m. For the first order derivatives, we obtain the following approximations

$$n_x(t) \approx D_0^{(1)} n(t) + \frac{\gamma}{d_n} n(x_0,t) s_0^f(t) e_1, \tag{3.2}$$

$$f_x(t) \approx D^{(1)} f(t) + f(x_{N+1},t) w, \tag{3.3}$$

$$m_x(t) \approx D_0^{(1)} m(t), \tag{3.4}$$

with

$$D^{(1)} = \Big[d_{i,j} \Big]_{i,j=0}^{N},$$

and $D_0^{(1)}$ being an $N+1$ by $N+1$ matrix with zeros in the first row and the other rows as in $D^{(1)}$, w is an $N+1$ by 1 column vector including the entries of the last column of D except the last entry $d_{N+1,N+1}$, e_1 is the unit $N+1$ by 1 column vector and

$$s_0^f(t) = \sum_{j=0}^{N+1} d_{0,j} f(x_j, t).$$

From (3.4), we obtain the approximation

$$\begin{bmatrix} \frac{\partial}{\partial x}\Big(n(x_0,t)\frac{\partial m}{\partial x}(x_0,t)\Big) \\ \frac{\partial}{\partial x}\Big(n(x_1,t)\frac{\partial m}{\partial x}(x_1,t)\Big) \\ \vdots \\ \frac{\partial}{\partial x}\Big(n(x_N,t)\frac{\partial m}{\partial x}(x_N,t)\Big) \end{bmatrix} \approx D^{(1)}\Big(n(t)\odot\Big(D^{(1)}m(t)\Big)\Big),$$

for the chemotaxis term in (2.1). Here, $\odot$ stands for the component-wise multiplication between two vectors. From (3.3) we obtain

$$\begin{bmatrix} \frac{\partial}{\partial x}\Big(n(x_0,t)\frac{\partial f}{\partial x}(x_0,t)\Big) \\ \frac{\partial}{\partial x}\Big(n(x_1,t)\frac{\partial f}{\partial x}(x_1,t)\Big) \\ \vdots \\ \frac{\partial}{\partial x}\Big(n(x_N,t)\frac{\partial f}{\partial x}(x_N,t)\Big) \end{bmatrix} \approx D^{(1)}\Big(n(t)\odot\Big(D^{(1)}f(t) + f(x_{N+1},t)w\Big)\Big),$$

for the haptotactic term. Considering the general case with the random motility coefficient $d_n = d_n(f,m)$, which may be a function of ECM or/and uPA, for the dispersion term in (2.1), from (3.2), we obtain the approximation

$$\begin{bmatrix} \frac{\partial}{\partial x}\Big(d_{n,0}(t)\frac{\partial n}{\partial x}(x_0,t)\Big) \\ \frac{\partial}{\partial x}\Big(d_{n,1}(t)\frac{\partial n}{\partial x}(x_1,t)\Big) \\ \vdots \\ \frac{\partial}{\partial x}\Big(d_{n,N}(t)\frac{\partial n}{\partial x}(x_N,t)\Big) \end{bmatrix} \approx \begin{array}{c} D^{(1)}\Big(d_n(t)\odot\Big(D_0^{(1)}n(t)+\frac{\gamma}{d_n}n(x_0,t)s_0^f(t)e_1\Big)\Big) \\ +d_{n,N}(t)s_{N+1}^n(t)w, \end{array}$$

where

$$d_n(t) = \begin{bmatrix} d_{n,0}(t) \\ d_{n,1}(t) \\ \vdots \\ d_{n,N}(t) \end{bmatrix},$$

$$d_{n,i}(t) = d_n(x_i, t),\ i = 0, 1, \ldots, N,$$

and

$$s^n_{N+1}(t) = \sum_{j=0}^{N+1} d_{N+1,j} n(x_j, t).$$

From (2.1) and the above three approximations, for the chemotaxis, haptotaxis, and dispersion terms, we obtain the following ordinary differential equation

$$\begin{aligned} \frac{dn}{dt}(t) &= D^{(1)}\left(d_n(t) \odot \left(D^{(1)}_0 n(t) + \frac{\gamma}{d_n} n(x_0, t) s^f_0(t) e_1 \right) \right) \\ &+ d_{n,N}(t) s^n_{N+1}(t) w - \chi D^{(1)}\left(n(t) \odot \left(D^{(1)} m(t) \right) \right) \\ &- \gamma D^{(1)}\left(n(t) \odot \left(D^{(1)} f(t) + f(x_{N+1}, t) w \right) \right) \\ &+ \mu_1 n(t) \odot p(t) \odot \Big(1 - n(t) - f(t) \Big). \end{aligned} \tag{3.5}$$

The discrete form for (2.2) is written in the following way

$$\frac{df}{dt}(t) = f(t) \odot \left(\mu_2 p(t) \odot \Big(1 - n(t) - f(t) \Big) - \eta m(t) \right). \tag{3.6}$$

The diffusion of the uPA can be approximated by

$$m_{xx}(t) \approx D^{(1)} m_x(t) + s^m_{N+1}(t) w,$$

which, from (3.4), gives

$$m_{xx}(t) \approx D^{(1)} D^{(1)}_0 m(t) + s^m_{N+1}(t) w$$

and results in the following discrete form for (2.3)

$$\frac{dm}{dt}(t) = d_m D^{(1)} D^{(1)}_0 m(t) + d_m s^m_{N+1}(t) w + \alpha n(t) - \beta m(t). \tag{3.7}$$

The system of ordinary differential equations (3.5), (3.6), (3.7), and (2.4) is not complete and has to be closed by initial conditions. From (2.5)-(2.6) we obtain

$$n(0) = \begin{bmatrix} \exp\big(-x_0^2/\epsilon\big) \\ \exp\big(-x_1^2/\epsilon\big) \\ \vdots \\ \exp\big(-x_N^2/\epsilon\big) \end{bmatrix} \tag{3.8}$$

and the starting vectors for the ECM and uPA are

$$f(0) = 1 - 0.5n(0), \quad m(0) = 0.5n(0), \tag{3.9}$$

respectively. The value $\epsilon = 0.01$ is chosen according to the laboratory data from Calvo et al. (2002) at the initial measurement. The initial conditions

$$p(0) = 1, \quad q(0) = 1$$

are chosen according to the numerical experiments with the semi-discrete scheme (3.5), (3.6), (3.7), (2.4), (3.8), and (3.9) and comparison of the numerical results with the laboratory data from Calvo et al. (2002).

The parameter values $\mu_1, \mu_2, \alpha, \beta, \gamma, \eta, \chi, d_n$, and d_m used in the model equations (2.1)-(2.3) and in the construction of the numerical scheme (3.5), (3.6), (3.7) are unknown and have to be estimated in order to find the approximations to the tumour cell density n, the ECM density f, and the uPA concentration m. In this paper, we apply the laboratory data from Calvo et al. (2002) to estimate the parameter values for the model (2.1)-(2.3).

The laboratory data from Calvo et al. (2002) are shown in Fig. 1 by $\triangleright$, $\diamond$, $+$, $\circ$, and $*$ for the *in vivo* tumour growth rates from the five prostate Pr14C1, Pr14C2, Pr117, Pr14, and Pr111 cell lines, respectively. For comparison, the numerical data are displayed by the solid curves. The laboratory data from Calvo et al. (2002) are compared with numerical data computed from the model equations (2.1)-(2.4) with various sets of values assigned for the constants $\mu_1, \mu_2, \alpha, \beta, \gamma, \eta, \chi, d_n$, and d_m. Each set of the constants gives a different solution n and among many solutions, for each prostate cell line, only the solutions which capture the main characteristic features of the *in vivo* tumour growth rates are chosen. This selection of solutions of the model equations (2.1)-(2.4) and their corresponding parameter values is computationally expensive and thus the design of the numerical algorithm is crucial in the estimations of the unknown parameters. Since our algorithm is based on spectrally accurate approximations for the partial derivatives with respect to x, instead of using large dimensional vectors, like e.g. in finite difference schemes, we use low dimensional vectors and save computational time for each solution computed for the selection of the parameter values.

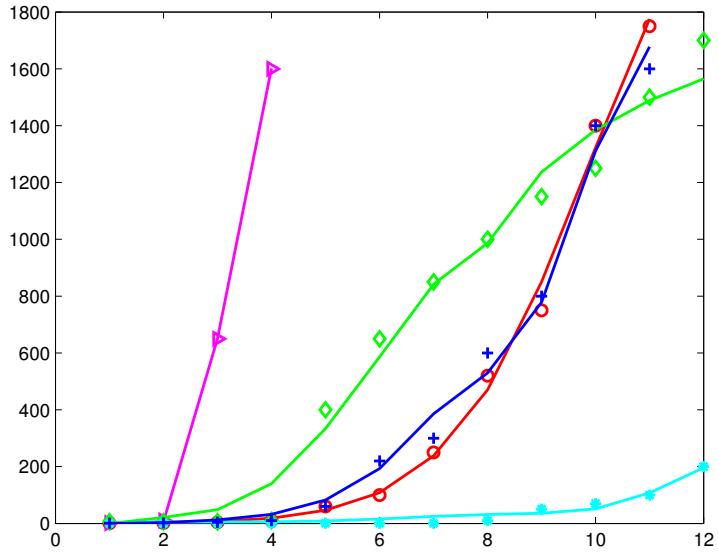

Figure 1. Laboratory versus numerical data. Laboratory data are denoted by $\triangleright$, $\diamond$, $+$, $\circ$, and $*$ for Pr14C1, Pr14C2, Pr117, Pr14, and Pr111 cell lines, respectively. Numerical data are represented by the solid curves

For each cell line, the parameter values are chosen according to the minimal error between the data and the computed values $v(t) = \frac{4}{3}\pi r^3(t)$, where

$$r(t) = k \int_0^1 n(x,t)dx,$$

and k is a constant of proportionality approximated by using the vertical scale from Figure 1I presented by Calvo et al. (2002). Here,

$$\int_0^1 n(x,t)dx \in [0,1]$$

corresponds with a mass of cells along a line segment scaled to the x-domain $[0,1]$, which is shifted in such a way that the tumours are centered around $x = 0$. The resulting parameter values are listed for each cell line in Table 1 and the solutions that correspond to these parameter values are presented in Fig. 1. As in Kolev and Zubik-Kowal (2011), we consider $x \in [0,1]$ for which $r(t) = k\int_0^1 n(x,t)dx$ corresponds with a mass of cells along a line segment in

1-dimensional x-domain and the volume is computed like in Kolev and Zubik-Kowal (2010) from $v(t) = \frac{4}{3}\pi r^3(t)$.

The curves from Fig. 1 show good correlations between the numerical and laboratory data for all the cell lines provided in Calvo et al. (2002). The strategies presented in this paper can also be used to predict *in vivo* tumour growth rates for other cell lines e.g. the mammary cancer cells considered in Jorcyk, Kolev and Zubik-Kowal (2011) (C3(1)/SV40 Large T-antigen (Tag) transgenic mouse model) and in Jorcyk et al. (2011) (spontaneous tumours of the mammary gland).

Table 1. Parameter values for *in vivo* cell growth in C3(1)Tag Mice.

Param.	Pr111	Pr117	Pr14	Pr14C2	Pr14C1
μ_1	$5.1 \cdot 10^{-1}$	$1.4 \cdot 10^{1}$	$4.6 \cdot 10^{2}$	$1.3 \cdot 10^{5}$	9.0
μ_2	$2.9 \cdot 10^{-4}$	$7.7 \cdot 10^{-9}$	$1.3 \cdot 10^{-14}$	$8.9 \cdot 10^{1}$	$2.9 \cdot 10^{-3}$
α	2.9	$7.8 \cdot 10^{-1}$	2.9	1.1	5.8
β	$3.5 \cdot 10^{-3}$	$8.4 \cdot 10^{-6}$	$3.7 \cdot 10^{-5}$	$9.1 \cdot 10^{-9}$	$3.8 \cdot 10^{-10}$
γ	$7.8 \cdot 10^{-3}$	$3.2 \cdot 10^{-9}$	$1.7 \cdot 10^{-9}$	$1.6 \cdot 10^{1}$	$3.7 \cdot 10^{-10}$
χ	$8.2 \cdot 10^{-11}$	$2.2 \cdot 10^{-3}$	$1.0 \cdot 10^{-7}$	$1.0 \cdot 10^{-4}$	$6.6 \cdot 10^{-4}$
η	$4.9 \cdot 10^{-2}$	$5.4 \cdot 10^{-1}$	$2.4 \cdot 10^{-1}$	$3.6 \cdot 10^{-1}$	2.0
d_n	$6.4 \cdot 10^{-3}$	$6.5 \cdot 10^{-2}$	$7.0 \cdot 10^{-2}$	$1.2 \cdot 10^{2}$	$2.8 \cdot 10^{-1}$
d_m	$8.7 \cdot 10^{-8}$	$1.9 \cdot 10^{-16}$	$3.2 \cdot 10^{-12}$	$2.2 \cdot 10^{-15}$	$1.5 \cdot 10^{-10}$

4. Concluding remarks and future directions

This paper shows that it is possible to construct mathematical models, which correlate with experimental data. We have applied the laboratory data from Calvo et al. (2002) and have estimated parameter values for the mathematical model of cancer cell invasion of tissue, which includes the chemotaxis, haptotaxis, and proliferation terms (see Chaplain and Lolas, 2006). The ability of the model to fit well the experimental data demonstrated in our paper confirms the usefulness of the mathematical modeling approach and the computational simulations in cancer research. In our future work we plan to develop the model for further investigations of mechanisms of cancer invasion and metastasis, which could be used for the design and improvement of treatment strategies.

Acknowledgements

The authors wish to express their gratitude to anonymous referees for the useful comments which led to the improvements in the presentation of the results.

References

Andreasen, P., Kjoller, L., Christensen, L. and Duffy, M. (1997) The urokinase-type plasminogen activator system in cancer metastasis: A review. *International Journal of Cancer* **72** (1), 1–22.

Andreasen, P., Egelund, R. and Petersen, H. (2000) The plasminogen activation system in tumor growth, invasion, and metastasis. *Cellular and Molecular Life Sciences* **57** (1), 25–40.

Bellomo, N. and Delitala, M. (2008) From the mathematical kinetic, and stochastic game theory to modelling mutations, onset, progression and immune competition of cancer cells. *Physics of Life Reviews* **5** (4), 183–206.

Bellomo, N. and Forni, G. (1994) Dynamics of tumor interaction with the host immune system. *Math. Comput. Modelling* **20** (1), 107–122.

Bellomo, N., Li, N. and Maini, P. (2008) On the foundations of cancer modelling: Selected topics, speculations, and perspectives. *Math. Models Methods Appl. Sci.* **18** (4), 593–646.

Canuto, C., Hussaini, M., Quarteroni, A. and Zang, T. (1998) *Spectral Methods in Fluid Dynamics*. Springer Verlag, New York.

Calvo, A., Xiao, N., Kang, J., Best, C., Leiva, I., Emmert-Buck, M., Jorcyk, C. and Green, J. (2002) Alterations in gene expression profiles during prostate cancer progression: functional correletions to tumorigenicity and down-regulation of selenoprotein-P in mouse and human tumors. *Cancer Research* **62** (18), 5325–5335.

Chaplain, M. and Anderson, A. (2003) *Mathematical modelling of tissue invasion. Cancer modelling and simulation*. Chapman & Hall/CRC Math. Biol. Med. Ser., Boca Raton, FL, 269–297.

Chaplain, M. and Lolas, G. (2006) Mathematical modelling of cancer invasion of tissue: dynamic heterogeneity. *Netw. Heterog. Media* **1** (3), 399–439.

De Angelis, E. and Lodz, B. (2008) On the kinetic theory for active particles: A model for tumor-immune system competition. *Math. Comput. Modelling* **47** (1-2), 196–209.

De Lillo, S., Salvatori, M. and Bellomo, N. (2007) Mathematical tools of the kinetic theory of active particles with some reasoning on the modelling progression and heterogeneity. *Math. Comput. Modelling* **45** (5-6), 564–578.

Fornberg, B. (1996) *A Practical Guide to Pseudospectral Methods*. Cambridge University Press, Cambridge.

Holzer, R., MacDougall, C., Cortright, G., Atwood, K., Green, J. and Jorcyk, C. (2003) Development and characterization of a progressive series of mammary adenocarcinoma cell lines derived from the C3(1)/SV40 large T-antigen transgenic mouse model. *Breast Cancer Research Treat* **77** (1), 65–76.

Jackiewicz, Z., Jorcyk, C., Kolev, M. and Zubik-Kowal, B. (2009) Correlation between animal and mathematical models for prostate cancer progression. *Comput. Math. Methods Med.* **10** (4), 241–252.

Jorcyk, C., Kolev, M. and Zubik-Kowal, B. (2011) *Mammary adenocarcinoma cell progression and numerical simulations. Integral Methods in Science and Engineering*, Springer, in press.

Jorcyk, C., Kolev, M., Tawara, K. and Zubik-Kowal, B. (2011) Experimental versus numerical data for breast cancer progression. In preparation.

Kolev, M. (2005) A mathematical model of cellular immune response to leukemia. *Math. Comput. Modelling* **41** (10), 1071–1081.

Kolev, M. and Zubik-Kowal, B. (2011) Numerical solutions for a model of tissue invasion and migration of tumour cells. *Journal of Biological Systems* **19** (1), 33-46.

Lachowicz, M. (2005) Micro and meso scales of description corresponding to a model of tissue invasion by solid tumours. *Math. Models Methods Appl. Sci.* **15** (11), 1667–1683.

Liotta, L., Rao, C. and Barsky, S. (1983) Tumour invasion and the extracellular matrix. *Lab. Invest.* **49** (6), 636–649.